

UC Irvine

UC Irvine Previously Published Works

Title

Analysis of novel alleles of brother of tout-velu, the drosophila ortholog of human EXTL3 using a newly developed FRT42D ovoD chromosome

Permalink

<https://escholarship.org/uc/item/6xz9x7hz>

Journal

Genesis, 54(11)

ISSN

1526-954X

Authors

Lujan, Ernesto
Bornemann, Douglas J
Rottig, Carmen
[et al.](#)

Publication Date

2016-11-01

DOI

10.1002/dvg.22981

Peer reviewed



HHS Public Access

Author manuscript

Genesis. Author manuscript; available in PMC 2017 November 01.

Published in final edited form as:

Genesis. 2016 November ; 54(11): 573–581. doi:10.1002/dvg.22981.

Analysis of novel alleles of *brother of tout-velu*, the *Drosophila* ortholog of human EXTL3 using a newly developed *FRT42D ovo^D* chromosome

Ernesto Lujan^{1,2,*}, Douglas J. Bornemann^{1,3,4,*}, Carmen Rottig⁵, Brian A. Bayless^{1,6}, Hugo Stocker⁵, Ernst Hafen⁵, Kavita Arora^{1,3,**}, and Rahul Warrior^{1,3,**}

Hugo Stocker: stocker@imsb.biol.ethz.ch; Ernst Hafen: hafen@imsb.biol.ethz.ch

¹Department of Developmental and Cell Biology, University of California Irvine, Irvine, CA 92697

³Developmental Biology Center, University of California Irvine, Irvine, CA 92697 ⁵Institute of Molecular Systems Biology, Auguste-Piccard-Hof 1, 8093 Zurich Switzerland

Abstract

The *FLP/FRT* system permits rapid phenotypic screening of homozygous lethal mutations in the context of a viable mosaic fly. Combining this system with *ovo^D* dominant female-sterile transgenes enables efficient production of embryos derived from mutant germline clones lacking maternal contribution from a gene of interest. Two distinct sets of *FRT* chromosomes, carrying either the mini-*white* (*w^{+mW.hs}*), or *rosy* (*ry⁺*) and *neomycin* (*neo^R*) transgenes are in common use. Parallel *ovo^D* lines were developed using the *w^{+mW.hs}* *FRT* insertions on the X and chromosomes 2R and 3L, as well as the *ry⁺*, *neo^R* *FRT* insertions on 2L and 3R. Consequently, mutations isolated on the X, 2R and 3L chromosomes in a *ry⁺*, *neo^R* *FRT* background, are not amenable to germline clonal analysis without labor-intensive recombination onto chromosome arms containing a *w^{+mW.hs}* *FRT*. Here we report the creation of a new *ovo^D* line for the *ry⁺*, *neo^R* *FRT* insertion at position *FRT42D* on chromosome 2R, through induced recombination in males. To establish the developmental relevance of this reagent we characterized the maternal-effect phenotypes of novel *brother of tout-velu* alleles generated on an *FRT42D* chromosome in a somatic mosaic screen. We find that an apparent null mutation that causes severe defects in somatic tissues has a much milder effect on embryonic patterning, emphasizing the necessity of analyzing mutant phenotypes at multiple developmental stages.

**Corresponding Authors: Rahul Warrior, Department of Developmental and Cell Biology, 4219 McGaugh Hall, Zot 2300, University of California, Irvine, Irvine CA 92697-2700, Phone: (949) 824-9798. Fax: (949) 824-4709. rwarrior@uci.edu. Kavita Arora, Department of Developmental and Cell Biology, 4215 McGaugh Hall, Zot 2300, University of California, Irvine, Irvine CA 92697-2700, Phone: (949) 824-1087. Fax: (949) 824-4709. karora@uci.edu.

²Current address: Department of Pathology, Harvard Medical School, Boston MA 02115. Ernesto_Lujan@hms.harvard.edu

⁴Current address: Department of Research and Development, University of Kansas, Lawrence, Kansas, dbornemann@ku.edu

⁶Current address: Department of Cell and Developmental Biology, University of Colorado-Anschutz Medical Campus, Denver, Colorado, BRIAN.BAYLESS@ucdenver.edu

*Co-first authors

Keywords

Drosophila FRT42D ovo^D; germline clonal analysis; *brother of tout-velu*, *botv*, EXTL3; N-acetylglucosamine transferase-II; heparan sulfate proteoglycan; HSPG

Introduction

The FLP/FRT system has been widely employed in *Drosophila* to generate clones of homozygous mutant tissue in an otherwise heterozygous animal (Dang and Perrimon, 1992; Golic, 1991; Golic and Lindquist, 1989; Griffin et al., 2014; Xu and Rubin, 1993; Xu and Rubin, 2012). This mosaicism enables analysis of mutant phenotypes at different developmental stages and in different tissues even if homozygosity for the mutation in the entire animal would be lethal. Further, the combination of FRT-mediated recombination with transgenes for the dominant *ovo^D* allele, which causes cell-autonomous degeneration of female germline cells, allows for efficient selection of mutant germline-clones and analysis of maternal-effect phenotypes (Chou et al., 1993; Perrimon and Gans, 1983). Flippase-induced FRT-mediated recombination in females transheterozygous for *ovo^D* and a mutation in a gene of interest results in mosaic ovaries, in which germline clones that lack *ovo^D* and are homozygous for the mutation survive to produce eggs, while all other germline cells are eliminated by *ovo^D*. Embryos derived from homozygous mutant eggs can be efficiently analyzed for germline and maternal-effect phenotypes (Chou and Perrimon, 1996).

Two distinct sets of pericentric FRT insertions that are in common use permit clonal analysis of greater than 95 percent of the *Drosophila* genome (Chou and Perrimon, 1996; Xu and Rubin, 1993). FRT inserts generated by Xu and Rubin are marked with *ry⁺*, *neo^R* while those created by Perrimon and co-workers are marked with *w^{+mW.hs}*. When *ovo^D*, FRT combinations were generated to facilitate germline mosaic analysis, parental FRT lines were chosen based on proximity of their FRT insertion to the centromere. *w^{+mW.hs}* FRT stocks were selected for the X chromosome, the right arm of the second chromosome (2R) and left arm of the third chromosome (3L), while the *ry⁺*, *neo^R* FRT inserts were used for autosomal arms 2L and 3R (Chou and Perrimon, 1996; Xu and Rubin, 1993). Thus corresponding *ovo^D* versions are lacking for the Xu and Rubin FRT inserts on the X chromosome (*FRT19A*), as well as chromosomal arms 2R (*FRT42D*), and 3L (*FRT80B*). Consequently, mutations generated on these FRT chromosomes cannot be analyzed for maternal-effect phenotypes without first going through the laborious process of recombining each mutation onto an FRT chromosome from the Chou and Perrimon set. Despite their obvious usefulness to the community, the underlying reason for the absence of these FRT *ovo^D* chromosomes is that they cannot be easily generated using standard genetic methods – females carrying *ovo^D* are sterile and meiotic recombination does not occur in *Drosophila* males. Additionally, transgenic lines for *ovo^D* genomic constructs are challenging to recover and complete expressivity of the dominant female-sterile phenotype likely requires the presence of multiple inserts (Chou et al., 1993). Here we report the creation of a new *FRT42D ovo^D* line using gamma irradiation induced male recombination. Furthermore, we demonstrate its functionality by characterizing maternal-effect phenotypes of novel alleles of *brother of tout-velu* (*botv*). The *botv* gene encodes an N-acetylglucosamine transferase-II (Han et al., 2004;

Kim et al., 2002; Takei et al., 2004) essential for synthesis of Heparan Sulfate Proteoglycan (HSPG) glycosaminoglycan (GAG) sugar chains.

Results and Discussion

To generate a novel *FRT42D ovo^D* chromosome, we used gamma irradiation to induce recombination in males (Bateman, 1968; Chou and Perrimon, 1996) that were transheterozygous for *P{neoFRT}42D* and *P{FRT(*w^{hs}*)}G13 P{*ovo^{D1-18}*}2R*. Briefly, potential recombinants were identified by resistance to G418, thus selecting for *P{neoFRT}42D*, as well as the presence of *w⁺* that marks the *ovo^D* transgene (see Methods). A total of four independent potential male recombinants were recovered from 380 surviving males and balanced stocks were established that allow for the maintenance of a dominant female-sterile (see Methods). We first confirmed the presence of *ovo^D* in the recombinant chromosome by assaying females from each stock for sterility. We also tested the ability of the *P{neoFRT}42D, P{ovo^{D1-18}}2R* chromosome (abbreviated *FRT42D ovo^D*) to produce clones in wing discs in combination with an *FRT42D* chromosome carrying a ubiquitously expressed GFP transgene (Fig. 1). The recovery of mitotic clones lacking GFP expression and neighboring twin spots showing high levels of GFP expression indicated that the *FRT42D* insert was functional.

Next we wished to determine whether the newly generated *FRT42D ovo^D* stock could be used successfully to recover mutant germline clones (GLCs). For this functional verification we first decided to use *botv^{A23}*, a previously characterized allele isolated on an *FRT42D* chromosome in a somatic mosaic screen for genes involved in patterning the adult wing (Takei et al., 2004). Botv acts together with the related Sister of tout velu (Sotv) and Tout velu proteins to polymerize GAG chains on HSPG core proteins, which are required for signaling by many growth factors. In humans mutations in the *ttv* and *sotv* homologs Ext1 and Ext2 result in Multiple Hereditary Exostoses a bone overgrowth syndrome (reviewed in (Busse-Wicher et al., 2014). Molecular characterization of the *botv^{A23}* allele, and the observation that wing disc clones homozygous for *botv^{A23}* display substantial loss of Hedgehog (Hh), Decapentaplegic and Wingless (Wg) activity, are both consistent with its classification as a strong loss-of-function allele (Takei et al., 2004). However, the lack of an *FRT42D, ovo^D* stock, has prevented examination of the maternal-effect phenotype of this allele. Null mutations in other *botv* alleles have been used to generate homozygous GLCs, and embryos lacking both maternal and zygotic activity (*M⁻Z⁻*) display a characteristic ‘lawn of denticles’ cuticle phenotype caused by impairment of heparan sulfate biosynthesis and consequent defects in Hh and Wg signaling pathways (Han et al., 2004; Takei et al., 2004). To generate mutant germline clones, recombination was induced in larvae heterozygous for *FRT42D botv^{A23}* and the newly generated *FRT42D ovo^D* chromosome, carrying a heat shock inducible Flippase transgene (*HS-FLP*). Adult female progeny were crossed to *FRT42D botv^{A23}* males to produce embryos that lacked both maternal and zygotic *botv* contributions (see Methods). As the males are heterozygous, only half of the GLCs derived embryos lack both maternal and zygotic *botv^{A23}* activity and are expected to display a mutant phenotype, while the remaining embryos fertilized by wild type sperm are paternally rescued to viability. As shown in Fig. 2A, B inviable *botv^{A23} M⁻Z⁻* embryos display fused denticle bands and reduced naked cuticle consistent with disruption of HSPG

biosynthesis and loss of Hh and Wg signaling, thus establishing the competence of the *FRT42D ovo^D* chromosome to generate GLCs.

We next used the *FRT42D ovo^D* chromosome to characterize the maternal contributions of six new *botv* alleles that were isolated in a genetic mosaic screen for growth regulating genes (Hafen, 2004). For this screen, EMS mutagenized *FRT42D* males were crossed to an eye-specific *eyeless*-Flippase (*ey-FLP*) driver and the progeny were analyzed for visible phenotypes resulting from altered growth of the mosaic mutant eye tissue (Fig. 3). Six independent mutations in *botv* were recovered, and the molecular identities of the lesions were determined by PCR amplification and sequencing of genomic DNA corresponding to the coding regions (summarized in Table 1; (Rottig et al., 2005). We used the newly generated *FRT42D ovo^D* line in combination with each of the six alleles to analyze the phenotypes resulting from loss of *botv* activity in *M⁻/Z⁻* embryos derived from GLCs. In each case, save one, we recovered embryos at the expected frequency that exhibited a characteristic loss of naked cuticle consistent with severe reduction of GAG polymerase activity (Fig. 2C–H).

Two of the newly isolated alleles, *botv^{VI.53}* and *botv^{VIII.28}* are missense mutations (Table 1, Fig. 4A). Of these, *botv^{VI.53}* is predicted to convert the first Aspartic acid (D) in the signature DXD motif of the putative nucleotide sugar-binding domain into an Asparagine (N) (Fig. 4C, red asterisk). This motif is conserved in all exostosin-like enzymes, and indeed, in a wide spectrum of UDP-sugar-dependent glycosyltransferases (Breton et al., 1998). The crystal structure of mouse ExtL2, a closely related enzyme, predicts that this motif helps coordinate a catalytic Mn²⁺ ion with the UDP sugar donor, and is therefore expected to be required for catalytic activity (Negishi et al., 2003; Pedersen et al., 2003). Consistent with this prediction, *M⁻/Z⁻* embryos derived from *botv^{VI.53}* GLCs exhibit a strong loss-of-function phenotype (Fig. 2C). In the second missense allele *botv^{VIII.28}* the Arginine⁸¹⁰ residue (R⁸¹⁰) in the catalytic domain is converted to a cysteine (C) (Fig. 2D and Fig. 4C, blue asterisk). All Botv orthologs examined, including orthologs from *Drosophila*, sea urchin, and human, contain an R in this position. However, this residue is not conserved in the paralogous GAG polymerase enzymes such as Ttv and Sotv (Fig. 4C, blue residues). Instead, all Sotv orthologs contain an oppositely charged glutamic acid (E) residue at this location. In Ttv orthologs a Threonine (T) is typically found in this position, although this conservation is not absolute (e.g. Valine in *Nasonia vitripennis* and Aspartic Acid in *Ciona intestinalis*, not shown). Therefore the R>C change in *botv^{VIII.28}* is likely to affect a Botv-specific characteristic of the catalytic domain. Analysis of *M⁻/Z⁻* embryos derived from GLCs of this allele using the *FRT42D ovo^D* stock reveals a moderately strong loss-of-function phenotype (see Fig. 2D) consistent with the importance of an R at position 810.

The remaining four alleles contain nonsense mutations that are predicted to result in truncated proteins lacking the entire catalytic domain (Fig. 4A and Table 1). Consistent with this premise, *M⁻/Z⁻* embryos derived from GLCs for three of the four alleles (*botv^{IX.21}*, *botv^{IX.42}*, and *botv^{2R37}*) produced cuticle phenotypes similar to null alleles (Fig. 2E–G). Surprisingly however, *botv^{2R24}*, which contains a stop codon at residue 50 and thus represents the best candidate for a null allele, produced embryos with a less severe cuticle

phenotype. These embryos display only partially fused denticle belts and retain some naked cuticle in each segment (Fig. 2H). To rule out the possibility that the weaker phenotype is due to a zygotic modifier in the background, we analyzed embryos derived from GLCs in *HS-FLP; FRT42D botv^{2R24}/FRT42D ovo^D* females crossed to males heterozygous for *botv⁴²³* (isolated in an independent screen on a different chromosomal background). The *botv⁴²³* mutation is also predicted to result in a protein lacking the catalytic domain (Takei et al., 2004), and, as we have shown above, *M⁻/Z⁻* embryos for this allele display a null phenotype (see Fig. 2B). We found that embryos derived from homozygous *botv^{2R24}* GLCs fertilized with *botv⁴²³* sperm (*M^{2R24/2R24}, Z^{2R24/423}*) also showed a cuticle phenotype that is less severe than *botv M⁻/Z⁻* nulls, comparable to *botv^{2R24} M⁻/Z⁻* (*M^{2R24/2R24}, Z^{2R24/2R24}*) animals (Fig. 2I, compare with 2H). Furthermore, embryos with mutant phenotypes were recovered at a frequency of 57% (n=49), while the remaining embryos were viable. This observation rules out the possibility that the milder *botv^{2R24}* GLC phenotype is caused by insufficient paternal rescue. Thus, despite the lethality of *botv^{2R24}* homozygotes and *botv^{2R24}* in *trans* to *botv* null alleles, analysis of GLC embryos indicates that Botv^{2R24} protein retains partial function.

Several mechanisms could account for the hypomorphic phenotype of *botv^{2R24} M⁻/Z⁻* embryos. For example, an alternative splicing event could eliminate the nonsense mutation in some fraction of transcripts. However, to preserve the signal-peptide transmembrane domain required for translocation into the endoplasmic reticulum (amino acids 57–76, Fig. 4B; (Kim et al., 2002), the alternate splice acceptor site would have to be located within approximately 20 nucleotides of the mutant codon. To examine this possibility, we performed RT-PCR on RNA isolated from wild type embryos using two forward primers complementary to the 5' untranslated regions (5' UTR) and a reverse primer complementary to a region downstream of the transmembrane domain (Fig. 4B). In each case, only a single product of a size consistent with the cDNA sequence reported in Flybase was observed. Parallel RT-PCR reactions performed with RNA isolated from *botv^{2R24} M⁻/Z⁻* embryos also produced single products indistinguishable in size from wild type (Fig. 5). Primers from the *sulfateless (stl)* gene were used as a control for RNA integrity (data not shown). This result argues that the mild phenotype of *botv^{2R24}* results from a mechanism other than alternative splicing. An alternative explanation for the less severe *botv^{2R24}* GLC phenotype could be occasional translational bypass of the nonsense stop codon. Low levels of stop-codon read-through have been shown to be phenotypically relevant in yeast and may depend in part on the regulation of translation termination factors as well as the nucleotide context of the stop codon (Bonetti et al., 1995; Namy et al., 2001; von der Haar and Tuite, 2007). Comparative genomics approaches to detect protein coding regions in 12 *Drosophila* species identified 283 potential examples of read-through of naturally occurring stop codons (Jungreis et al., 2011), while ribosome profiling assays have identified an additional 300 read through events in *D. melanogaster* (Dunn et al., 2013). An intriguing third possibility is that the *botv* transcript may contain an Internal Ribosome Entry Site (IRES) within the coding region upstream of the transmembrane domain capable of initiating translation at an AUG downstream of the nonsense Figure 5. RT-PCR analysis does not indicate the presence of alternative splicing in ***botv^{2R24}* embryos**

Agarose gel stained with ethidium bromide showing RT-PCR products from wild type and *botv*^{2R24} *M⁻/Z⁻* (or *M*^{2R24/2R24}, *Z*^{2R24/423}) mutant embryos. Forward primers (F1 and F2) and a single reverse primer (R1) downstream of the codon affected in *botv*^{IX.21} and the transmembrane domain were used (marked in Fig. 4B). Both the wild type and *botv*^{2R24} *M⁻/Z⁻* embryos show PCR products of the expected sizes (451 bp for F2-R1, and 540 bp for the F1-R1 primer pairs). No amplicons corresponding to alternatively spliced transcripts were detected in GLC derived embryos.

mutation. IRESes have already been shown to exist in the 5' UTRs of *ttv* and *sulfateless* (*sfl*) another enzyme required for heparan sulfate biosynthesis. Furthermore, the 5' UTRs of a large percentage of GAG biosynthetic enzymes from multiple species are exceptionally long with multiple upstream AUG codons, consistent with the possibility they may contain IRES elements as well (Bornemann et al., 2008). Although the 5' UTR from the *botv* transcript is not unduly long, it contains two upstream AUGs, one of which creates a potential upstream ORF. We note that even if the *botv* transcript contains IRES activity, it is not by itself sufficient to rescue embryos from homozygous mutant GLCs to viability, suggesting either that cap-dependent translation predominates, or that the mutation somehow compromises the IRES function.

In summary, here we describe the generation and characterization of an *FRT42D ovo*^D line on the right arm of the second chromosome. This line will facilitate analysis of the maternal and early embryonic functions of the large number of mutations isolated in screens using the *FRT42D* background (for example (Chen et al., 2005; Kagey et al., 2012; Pressman et al., 2012), through efficient generation of GLCs. We have demonstrated the utility of this line through analysis of a series of *botv* alleles isolated in a somatic screen for factors affecting eye development. Ironically, while five of six *botv* alleles examined behave as strong loss-of-function alleles in GLC analysis, the best candidate for a null allele based on sequence data displays a hypomorphic GLC phenotype. This result underscores the importance of examining, where possible, both early maternal-effect phenotypes, as well as late somatic phenotypes when characterizing novel mutations, a process made feasible for mutations on the *FRT42D* background by generation of the *FRT42D ovo*^D line described here.

METHODS

Drosophila Stocks and Male recombination

FRT42D, *botv*⁴²³ flies were kindly provided by T. Tabata (University of Tokyo). All other stocks were obtained from the Bloomington Stock Center (Indiana University, Bloomington, Indiana).

For gamma-ray induced male recombination, males of the genotype *FRTG13 ovo*^D (*P*{*FRT*(*w*^{hs})}*G13 P*{*ovoD1-18*}*2R/T(1;2)OR64/CyO*) were mated with *FRT42D* (*P*{*ry*[+*t7.2*]=*neoFRT*}*42D; ry*[*605*]) females in plastic vials for 24 hours and the adults removed. The resulting larvae were allowed to mature for 48–72 hours at 25°C before the vials were gamma irradiated at a dose of 0.561 rads per minute for 3–4 minutes using a Cs137 source (KS ERI Isomedix). Irradiated males that eclosed were singly mated to *w⁻/w⁻; CyO; TM3/ap^{Xa}* virgins to recover potentially mutant chromosomes over the *CyO* balancer.

Progeny were raised on G418 food to eliminate animals with the *FRTG13* chromosome and select for lines with the *FRT42D* insert, which carries neomycin resistance. G418-resistant adult male progeny were scored for presence of *w⁺*, which marks the *ovo^D* transgene. Due to the close chromosomal proximity of *FRTG13* and *FRT42D* insertion sites, recombinants between the two loci are expected to be extremely rare. Analysis of 380 surviving males yielded four independent potential male recombinants. *w⁺* males were mated to *w⁻/w⁻; OR64/CyO; TM3* females to create stable stocks. The presence of *OR64* a dominant male lethal in the stock ensures that only *ovo^D* males and *OR64* females contribute to the next generation. Each of these lines was functionally assayed for the presence of the *ovo^D* insert (female sterility), as well as the ability to generate mitotic and germline clones in conjunction with an *FRT42D* chromosome.

G418 selection

G418 media was produced by mixing a G418 stock solution with molten standard cornmeal fly food at 70°C, to achieve a final concentration of 1 mg/ml G418. Green food coloring was added simultaneously to assess even distribution and mixing. 25 ml of food was dispensed into each vial and stored at 4°C until used.

Wing disc, eye disc and germline clones

Flies carrying the *FRT42D ovo^D* line as well as a heat-shock inducible Flippase transgene on the X chromosome were crossed to an *FRT42D* line carrying a ubiquitin-driven GFP transgene. Mosaic wing disc clones were generated essentially as described previously (Bornemann et al., 2004). Mosaic flies with mutant eyes and head capsules were generated using the ey-FLP/FRT technique essentially as described in (Newsome et al., 2000). To generate germ line clone embryos *HS-FLP; FRT42D ovo^D/CyO* males were mated to *y⁻ w⁻; FRT42D botv^{*}/CyO, KrGFP* females; eggs were collected for two days, parents were removed and Flippase expression was induced at first and second instar stages by heat shocking larvae in food vials in a 37°C water bath for 1 hour on two consecutive days. *Cy⁺* female progeny were crossed to appropriate *y⁻ w⁻; FRT42D botv^{*}/CyO, KrGFP* males. Embryos were collected on standard apple juice agar plates, and the chorion was manually removed. 10–20 dechorionated embryos were mounted on a glass slide in 30 µl of 1:1 lactic acid: Hoyer's solution and incubated at 65°C overnight prior to analysis and photography.

RT-PCR

botv^{2R24} M⁻Z⁻ embryos were obtained from *y⁻, w⁻, HS-FLP; FRT42D ovo^D/FRT42D botv^{2R24}* mosaic mothers mated to *FRT42D botv^{2R24}/CyO, Kr-Gal4, UAS-GFP* males. 250–500 wild type and *botv^{2R24}* mutant embryos were collected overnight on standard apple-juice agar plates and dechorionated for 2 minutes in 50% bleach. Embryos lacking GFP expression were selected using a Leica MZFLIII fluorescence microscope equipped with a GFP filter. 250–500 embryos were homogenized in microfuge tubes using plastic pestles (Contes) in 35 µl of 1% beta-mercaptoethanol-supplemented lysis buffer from the RNA Easy kit (Qiagen). Homogenates were centrifuged at maximum speed for 3 minutes, the supernatants transferred to a new tube, mixed with 350 µl of 70% ethanol, and passed through the RNA Easy mini-column. RNA recovered according to the manufacturer's directions. RNA integrity was checked on a 0.7% agarose gel, and 1 µl of RNA was used as

template for RT-PCR using the OneStep RT-PCR kit (Qiagen). The parameters used were: 30 minute incubation with reverse transcriptase, followed by denaturation at 95°C (15 min.), 35 cycles of denaturation at 95°C (1 min.), annealing at 55°C (1 min.) and extension at 72°C (1 min.), with a final 10 min. incubation at 72°C for complete extension. The following primers were used: botvF1 5' CTCCACTCGCGATAAAG 3', botvF2 5' CATTCCGGAGAGGCGTA 3', botvR1 5' CTGTTTGCTCCCTAAGC 3', SfIF1 5' CAACAAAGTGTGTTCCGAGCC 3', SfIR1 3' CGATATTGTCATATTGTCGTC 3'.

Acknowledgments

Grant Support: National Institutes of Health grants GM-71476 and GM-067247 to RW. EL and BAB were supported by R25GM055246 and T34GM069337.

This work was supported by National Institutes of Health grants GM-71476 and GM-067247 to RW. EL was supported by R25GM055246 and T34GM069337. The *FRT42D*, *ovo^D* stock generated in this study will be made available to the research community.

References

- Bateman AJ. The influence of dose and germ-cell stage on x-ray-induced crossovers in male *Drosophila*. *Mutat Res.* 1968; 5:243–257. [PubMed: 5672970]
- Bonetti B, Fu L, Moon J, Bedwell DM. The efficiency of translation termination is determined by a synergistic interplay between upstream and downstream sequences in *Saccharomyces cerevisiae*. *J Mol Biol.* 1995; 251:334–345. [PubMed: 7650736]
- Bornemann DJ, Duncan JE, Staatz W, Selleck S, Warrior R. Abrogation of heparan sulfate synthesis in *Drosophila* disrupts the Wingless, Hedgehog and Decapentaplegic signaling pathways. *Development.* 2004; 131:1927–1938. [PubMed: 15056609]
- Bornemann DJ, Park S, Phin S, Warrior R. A translational block to HSPG synthesis permits BMP signaling in the early *Drosophila* embryo. *Development.* 2008; 135:1039–1047. [PubMed: 18256192]
- Bretton C, Bettler E, Joziassse DH, Geremia RA, Imberty A. Sequence-function relationships of prokaryotic and eukaryotic galactosyltransferases. *J Biochem.* 1998; 123:1000–1009. [PubMed: 9603985]
- Busse-Wicher M, Wicher KB, Kusche-Gullberg M. The exostosin family: proteins with many functions. *Matrix Biol.* 2014; 35:25–33. [PubMed: 24128412]
- Chen J, Call GB, Beyer E, Bui C, Cespedes A, Chan A, Chan J, Chan S, Chhabra A, Dang P, Deravanesian A, Hermogeno B, Jen J, Kim E, Lee E, Lewis G, Marshall J, Regalia K, Shadpour F, Shemmassian A, Spivey K, Wells M, Wu J, Yamauchi Y, Yavari A, Abrams A, Abramson A, Amado L, Anderson J, Bashour K, Bibikova E, Bookatz A, Brewer S, Buu N, Calvillo S, Cao J, Chang A, Chang D, Chang Y, Chen Y, Choi J, Chou J, Datta S, Davarifar A, Desai P, Fabrikant J, Farnad S, Fu K, Garcia E, Garrone N, Gasparyan S, Gayda P, Goffstein C, Gonzalez C, Guirguis M, Hassid R, Hong A, Hong J, Hovestreydt L, Hu C, Jamshidian F, Kahen K, Kao L, Kelley M, Kho T, Kim S, Kim Y, Kirkpatrick B, Kohan E, Kwak R, Langenbacher A, Laxamana S, Lee C, Lee J, Lee SY, Lee TH, Lee T, Lezcano S, Lin H, Lin P, Luu J, Luu T, Marrs W, Marsh E, Min S, Minasian T, Misra A, Morimoto M, Moshfegh Y, Murray J, Nguyen C, Nguyen K, Nodado E 2nd, O'Donahue A, Onugha N, Orjiakor N, Padhiar B, Pavel-Dinu M, Pavlenko A, Paz E, Phaklides S, Pham L, Poulouse P, Powell R, Pusic A, Ramola D, Ribbens M, Rifai B, Rosselli D, Saakyan M, Saarikoski P, Segura M, Singh R, Singh V, Skinner E, Solomin D, Soneji K, Stageberg E, Stavchanskiy M, Tekchandani L, Thai L, Thiyaratnam J, Tong M, Toor A, Tovar S, Trangsrud K, Tsang WY, Uemura M, Unkovic M, Vollmer E, Weiss E, Wood D, Wu S, Wu W, Xu Q, Yackle K, Yarosh W, Yee L, Yen G, Alkin G, Go S, Huff DM, Minye H, Paul E, Villarasa N, Milchanowski A, Banerjee U. Discovery-based science education: functional genomic dissection in *Drosophila* by undergraduate researchers. *PLoS biology.* 2005; 3:e59. [PubMed: 15719063]

- Chou TB, Noll E, Perrimon N. Autosomal P[*ovo^{DI}*] dominant female-sterile insertions in *Drosophila* and their use in generating germ-line chimeras. *Development*. 1993; 119:1359–1369. [PubMed: 8306893]
- Chou TB, Perrimon N. The autosomal FLP-DFS technique for generating germline mosaics in *Drosophila melanogaster*. *Genetics*. 1996; 144:1673–1679. [PubMed: 8978054]
- Dang DT, Perrimon N. Use of a yeast site-specific recombinase to generate embryonic mosaics in *Drosophila*. *Dev Genet*. 1992; 13:367–375. [PubMed: 1292893]
- Dunn JG, Foo CK, Belletier NG, Gavis ER, Weissman JS. Ribosome profiling reveals pervasive and regulated stop codon readthrough in *Drosophila melanogaster*. *Elife*. 2013; 2:e01179. [PubMed: 24302569]
- Golic KG. Site-specific recombination between homologous chromosomes in *Drosophila*. *Science*. 1991; 252:958–961. [PubMed: 2035025]
- Golic KG, Lindquist S. The FLP recombinase of yeast catalyzes site specific recombination in the *Drosophila* genome. *Cell*. 1989; 59:499–509. [PubMed: 2509077]
- Griffin R, Binari R, Perrimon N. Genetic odyssey to generate marked clones in *Drosophila* mosaics. *Proceedings of the National Academy of Sciences of the United States of America*. 2014; 111:4756–4763. [PubMed: 24623854]
- Hafen E. Cancer, type 2 diabetes, and ageing: news from flies and worms. *Swiss Med Wkly*. 2004; 134:711–719. [PubMed: 15635489]
- Han C, Belenkaya TY, Khodoun M, Tauchi M, Lin X, Lin X. Distinct and collaborative roles of *Drosophila* EXT family proteins in morphogen signalling and gradient formation. *Development*. 2004; 131:1563–1575. [PubMed: 14998928]
- Jungreis I, Lin MF, Spokony R, Chan CS, Negre N, Victorsen A, White KP, Kellis M. Evidence of abundant stop codon readthrough in *Drosophila* and other metazoa. *Genome Res*. 2011; 21:2096–2113. [PubMed: 21994247]
- Kagey JD, Brown JA, Moberg KH. Regulation of Yorkie activity in *Drosophila* imaginal discs by the Hedgehog receptor gene patched. *Mech Dev*. 2012; 129:339–349. [PubMed: 22705500]
- Kim BT, Kitagawa H, Tamura Ji J, Kusche-Gullberg M, Lindahl U, Sugahara K. Demonstration of a novel gene DEXT3 of *Drosophila melanogaster* as the essential N-acetylglucosamine transferase in the heparan sulfate biosynthesis: chain initiation and elongation. *The Journal of biological chemistry*. 2002; 277:13659–13665. [PubMed: 11832488]
- Namy O, Hatin I, Rousset JP. Impact of the six nucleotides downstream of the stop codon on translation termination. *EMBO reports*. 2001; 2:787–793. [PubMed: 11520858]
- Negishi M, Dong J, Darden TA, Pedersen LG, Pedersen LC. Glucosaminylglycan biosynthesis: what we can learn from the X-ray crystal structures of glycosyltransferases GlcAT1 and EXTL2. *Biochem Biophys Res Commun*. 2003; 303:393–398. [PubMed: 12659829]
- Newsome TP, Asling B, Dickson BJ. Analysis of *Drosophila* photoreceptor axon guidance in eye-specific mosaics. *Development*. 2000; 127:851–860. [PubMed: 10648243]
- Papadopoulos JS, Agarwala R. COBALT: constraint-based alignment tool for multiple protein sequences. *Bioinformatics*. 2007; 23:1073–1079. [PubMed: 17332019]
- Pedersen LC, Dong J, Taniguchi F, Kitagawa H, Krahn JM, Pedersen LG, Sugahara K, Negishi M. Crystal structure of an alpha 1,4-N-acetylhexosaminyltransferase (EXTL2), a member of the exostosin gene family involved in heparan sulfate biosynthesis. *The Journal of biological chemistry*. 2003; 278:14420–14428. [PubMed: 12562774]
- Perrimon N, Gans M. Clonal analysis of the tissue specificity of recessive female-sterile mutations of *Drosophila melanogaster* using a dominant female-sterile mutation Fs(1)K1237. *Developmental biology*. 1983; 100:365–373. [PubMed: 6418585]
- Pressman S, Reinke CA, Wang X, Carthew RW. A Systematic Genetic Screen to Dissect the MicroRNA Pathway in *Drosophila*. *G3 (Bethesda)*. 2012; 2:437–448. [PubMed: 22540035]
- Rottig C, Stocker H, Nairz K, Rintelen F, Oldham S, Hafen E. Identification of novel genes regulating growth in *Drosophila*. *Annual Drosophila Research Conference*. 2005; 46:463A.
- Takei Y, Ozawa Y, Sato M, Watanabe A, Tabata T. Three *Drosophila* EXT genes shape morphogen gradients through synthesis of heparan sulfate proteoglycans. *Development*. 2004; 131:73–82. [PubMed: 14645127]

- von der Haar T, Tuite MF. Regulated translational bypass of stop codons in yeast. *Trends Microbiol.* 2007; 15:78–86. [PubMed: 17187982]
- Xu T, Rubin GM. Analysis of genetic mosaics in developing and adult *Drosophila* tissues. *Development.* 1993; 117:1223–1237. [PubMed: 8404527]
- Xu T, Rubin GM. The effort to make mosaic analysis a household tool. *Development.* 2012; 139:4501–4503. [PubMed: 23172911]

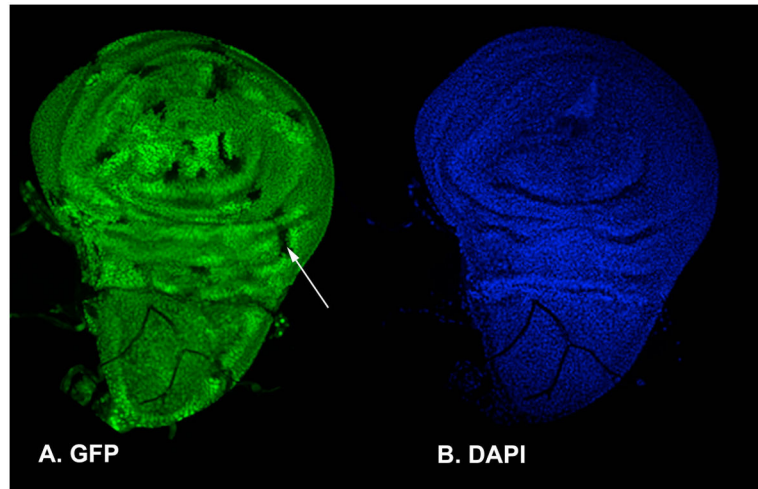


Figure 1. The novel *FRT42D ovo^D* chromosome effectively generates somatic wing disc clones Male *FRT42D ovo^D* flies carrying a heat-shock inducible Flippase transgene on the X chromosome were crossed to females from an *FRT42D* line carrying a GFP transgene under control of the *ubiquitin* promoter. Larvae were heat-shocked at first and second instar stages to induce Flippase expression. (A) Third instar wing disc showing clones of cells lacking GFP expression (arrow) adjacent to twin-spots expressing high levels of GFP (intense green). (B) Same disc as in A visualized using the DAPI channel to show tissue integrity.

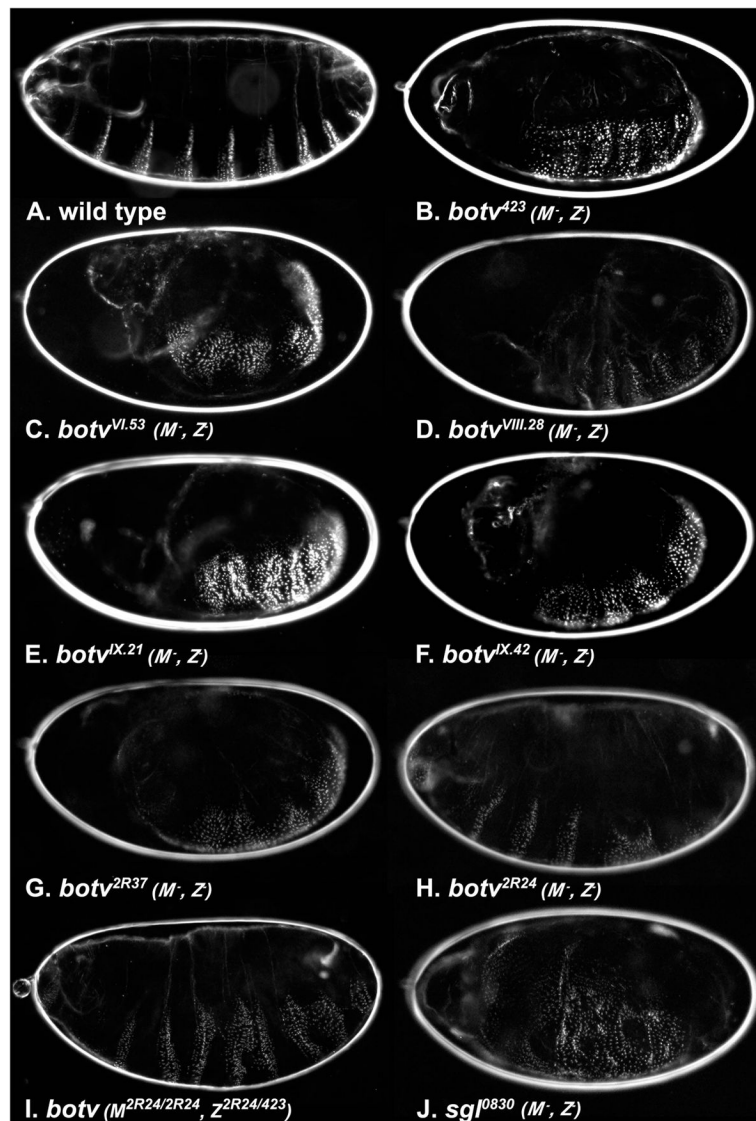


Figure 2. Germline clones generated using the *FRT42D ovo^D* chromosome
 Cuticle preparations of wild type (A) and mutant embryos derived from germ line clones (B–J). (B–I) *FRT42D ovo^D/CyO* males carrying an X-linked heat-shock inducible Flippase transgene were mated with females carrying a *FRT42D* chromosome bearing a specific *botv* allele/*CyO*. Progeny were heat-shocked to induce Flippase expression and allowed to develop to adulthood. Straight-winged females were selected and backcrossed to males heterozygous for the same mutant allele (B–H), or for *botv⁴²³*, which was isolated on an unrelated chromosomal background (I). To eliminate paternally rescued individuals (through hatching), GLC embryos were recovered and allowed to develop for two days at room temperature prior to mounting. (J) Embryo derived from females with homozygous *sgl⁰⁸³⁰* germ line clones, mated with heterozygous *sgl^{0830/+}* males.

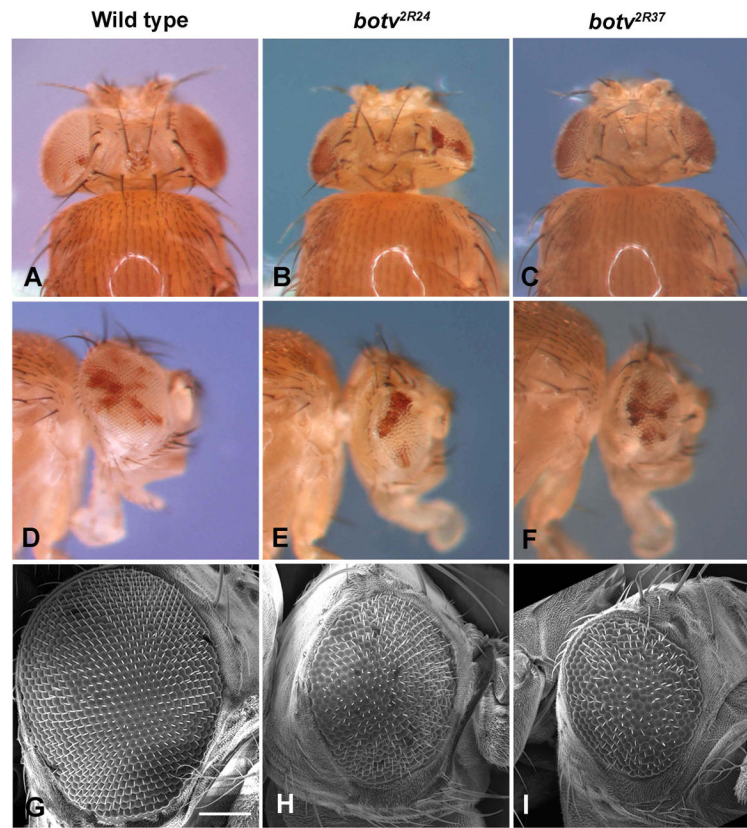


Figure 3. Loss of *botv* activity results in reduced growth of eye tissue

Dorsal (A–C) and lateral (D–F; G–I) views of mosaic heads generated using the ey-FLP/FRT system. A–F are light microscope images while G–I are scanning electron micrographs. Eyes and heads largely homozygous for either *botv*^{2R24} (B, E, H) or *botv*^{2R37} (C, F, I) display a marked reduction in size compared to control (A, D, G) mosaic heads generated with the isogenized FRT42D chromosome used in the genetic screen.

A. Botv domain structure



B. Botv N-terminus

agccctgcatcgcggttgccaacgaaacggactccactcgcgataaaagtgtaaataaatga
 gatattttggtggaatcgcgagctgaaactaatgccatgcccaccggcgtacgaccttggc
 cattccggagagggcgtaaccaaccctggacactggcagcggcgcgaaacgaagcctgt
 H S G E A Y Q P L D T G S G G G N E A C
 gccccgaactcatcctccgcgcaaactccgccattcgatgggattccggacatcctggatg
 A P N S S S A Q I R H S M G F R T S W M
 cggcagttccgcgctacaaactgccatgggtgctgctgatgctgctgtttctcgtttcc
 R Q F R R Y K L P M V L L M L L F L V S
 tgcctagcataccgcatcctaagcgtggagcaagatgccccgccactggatctgcatcgt
 C L A Y R I L S V E Q D A P P L D L H R
 agttcaccgctagatgctcgaagatttcagcgcctatgagagcaggagatcgtgaaa
 S S P L L D A Y E D F S A M R A G D L K
 atgcgcatcgaggagatggttagaatcaagagcaccgtgtccgtggagttgcgcgaaattg
 M R I E E M V R I K S T V S V E L R E L
 gagtcccgtcgccagaagctgcaatcgacattagccagtacaaccagaagatcgaggag
 E S R R Q K L Q S D I S Q Y N Q K I E E
 ctcaaacggaactgcttagggagcaaacagaactggagcgcctcaagatctcctggtggag...
 L K Q E L L R E Q T E L E R L K I S V E...
 Primer F1
 Primer F2
 Primer R1

C. Catalytic Domain Alignments

<i>Ext21 MM</i>	-PQTANKMRNRLQVFEVETNAVLMVDDDTL-ISAQDLVFAF [*] SIWQQFPDQIIGFVPRKHVSTS-SGIYSYGGFELQTPG	202
<i>Ext13 HS</i>	-RTEKNSLNNRFLPWNEIETEALSLIDDDAH-LRHDEIMFGFRVWREARDRIVGFPGRYHAWDI--PHQSWLYNSNY--	792
<i>Ext13 XT</i>	-RTEKNSLNNRFLPWDQIETEAVLSIDDDAH-LRHDEIMFGFRVWREARDRIVGFPGRYHAWDI--PHRSWLYNSNY--	792
<i>Ext13 SP</i>	-KTTVNSLNNRFLPYDEIETEALSLIDDDAH-LRHDEILFGFRVWRESRDRVVGFPGRYHAWDL-NYRNGFLYSANYS--	821
<i>Botv DM</i>	-RAPRNSLNNRFLPFVDIETEAVLSVDDDAH-LRHDEILFGFRVWREHRDRVVGFPGRYHAWDLGNPQGWHYNSNY--	845
<i>Botv DW</i>	-RAPRNSLNNRFLPFVDIETEAVLSVDDDAH-LRHDEILFGFRVWREHRDRVVGFPGRYHAWDLSS--NNMWHYNSNY--	811
<i>Ext1 HS</i>	-EGESKVMSSRFLPYDNIITDAVLSLDEDTV-LSTTEVDFAFTVWQSFPERIVGYPARSHFWDN--SKERWGYTSKWT--	613
<i>Ext1 XT</i>	-EGESKVMSSRFLPYDNIITDAVLSLDEDTV-LSTTEVDFAFTVWQSFPERIVGYPARSHFWDN--AKERWGYTSKWT--	605
<i>Ext1 CI</i>	-DDQPKTMGRFLPR-QFTTDAI LSLDDVDM-LNSQEI D F A F D V W R S F P D R I V G F P A R S H F W N S -- S K S K W V Y T S K W S --	629
<i>Ttv DM</i>	TTEGRPSISQRFLPYDEIQTDVAVLSLDEDAI-LNTDELDFAYTVWRDFPERIVGYPARAHFWDN--SKNAWGYTSKWT--	629
<i>Ttv DW</i>	TTEGRPSISQRFLPYDEIQTDVAVLSLDEDAI-LNTDELDFAYTVWRDFPERIVGYPARAHFWDN--SKNAWGYTSKWT--	645
<i>Ext2 HS</i>	-RTAENKLSNRFFPYDEIETEAVLAIDDDIIMLTSDQLQFGEVWREFPDRLVGYPGRHLHWDH--EMNKWYSESWT--	587
<i>Ext2 XT</i>	-KTTENKLSNRFFPYSEIETEAVLAIDDDIIMLTSDQLQFGEVWREFPDRLVGYPGRHLHWDH--EMSKWYSESWT--	587
<i>Sotv DM</i>	-QTKENKLSNRFFPYPEIETEALITIDDDIIMLTDELDFGEVWREFPDHIVGFPRIHVWEN--VTMRWHYSESWT--	586
<i>Sotv DW</i>	-QTQENKLSNRFFPYPEIETEALITIDDDIIMLTDELDFGEVWREFPDHIVGFPRIHVWEN--VTMRWHYSESWT--	597

Figure 4. Molecular lesions in novel mutations in the *botv* locus

(A) Domain structure of the Botv protein showing the transmembrane domain (gold), and the glycosyltransferase catalytic domain (red). The relative locations of the nonsense (*botv*^{2R24}, *botv*^{IX.21}, *botv*^{IX.42}, *botv*^{2R37}) and missense (*botv*^{VI.53} and *botv*^{VIII.28}) mutations are indicated. (B) N-terminal sequence of the *botv* transcript with predicted protein in single-letter code. The putative transmembrane domain is depicted in gold. Codons affected by mutations *botv*^{2R24} (CAG to TAG) and *botv*^{IX.21} (CAA to TAA) are marked and underlined in red. The predicted start codon and a possible IRES-mediated alternative start codon are depicted and underlined in green. RT-PCR primers are indicated by arrows. (C) Alignment of the catalytic glycosyltransferase domains from Botv, Ttv and Sotv orthologs in multiple organisms using COBALT (Papadopoulos and Agarwala, 2007). The DXD Mn²⁺ metal ion coordination motif is in red. The red asterisk indicates the amino acid affected by

the *botv*^{VI.53} mutation (D to N). Blue highlighting and the blue asterisk indicate the amino acid altered by the *botv*^{VIII.28} mutation (R to C). The names and species abbreviations of Botv orthologs are in dark blue, Ttv orthologs in gold and Sotv orthologs in green. Ext2L is a related glycosyltransferase for which the catalytic domain crystal structure has been solved. Note the absolute conservation of the residue affected in *botv*^{VIII.28}, as an R in Botv homologs and as an oppositely charged E in Sotv orthologs. Species abbreviations are as follows: *MM*, *Mus musculus* (mouse); *HS*, *Homo sapiens* (human); *XT*, *Xenopus tropicalis* (frog); *SP*, *Strongylocentrotus purpuratus* (sea urchin); *CI*, *Ciona intestinalis* (sea squirt); *DM*, *Drosophila melanogaster*, *DW* *Drosophila willistoni*.

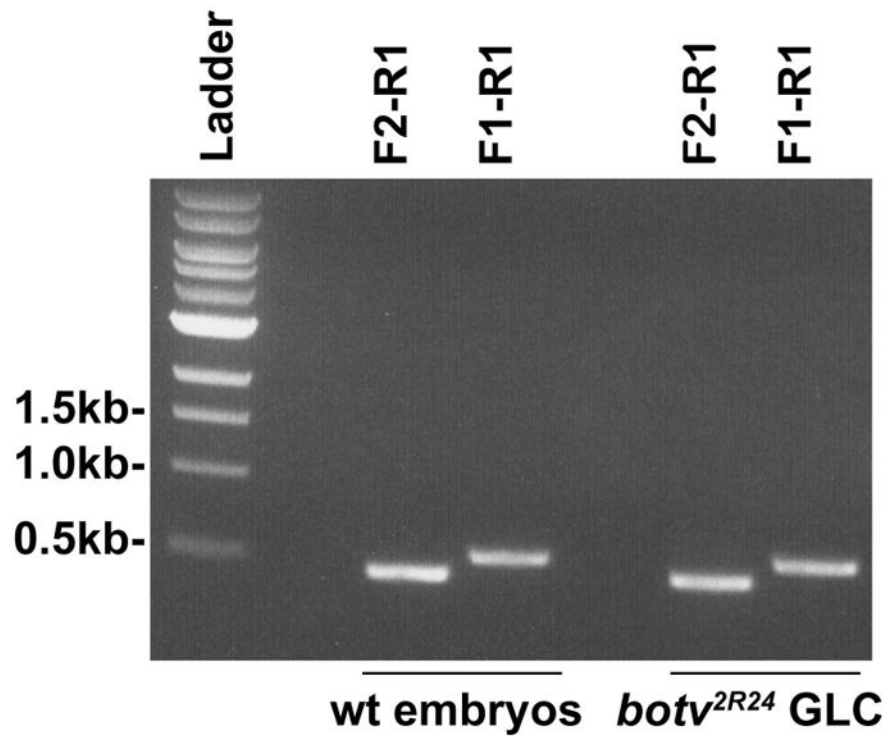


Figure 5. RT-PCR analysis does not indicate the presence of alternative splicing in *botv*^{2R24} embryos

Agarose gel stained with ethidium bromide showing RT-PCR products from wild type and *botv*^{2R24} *M*⁻/*Z*⁻ (or *M*^{2R24/2R24}, *Z*^{2R24/423}) mutant embryos. Forward primers (F1 and F2) and a single reverse primer (R1) downstream of the codon affected in *botv*^{IX.21} and the transmembrane domain were used (marked in Fig. 4B). Both the wild type and *botv*^{2R24} *M*⁻/*Z*⁻ embryos show PCR products of the expected sizes (451 bp for F2-R1, and 540 bp for the F1-R1 primer pairs). No amplicons corresponding to alternatively spliced transcripts were detected in GLC derived embryos.

Table 1Molecular lesions in *botv* alleles

Mutant allele	Codon altered	Predicted effect on protein
<i>2R24</i>	CAG to TAG	Nonsense: Q 50 to Stop
<i>IX.21</i>	CAA to TAA	Nonsense: Q 136 to Stop
<i>IX.42</i>	CGA to TGA	Nonsense: R 242 to Stop
<i>2R37</i>	CAA to TAA	Nonsense: Q 474 to Stop
<i>VI.53</i>	GAC to AAC	Missense: D 795 to N
<i>VIII.28</i>	CGT to TGT	Missense: R 810 to C

Author Manuscript

Author Manuscript

Author Manuscript

Author Manuscript